ACS OMEGA

Article

Cite This: ACS Omega 2019, 4, 20882−20893

http://pubs.acs.org/journal/acsodf

Molecular and Cellular Response of Co-cultured Cells toward Cobalt Chloride ($CoCl_2$)-Induced Hypoxia

Vinay Kumar Tripathi,[†,§] Sivakumar Allur Subramaniyan,[†,‡,§] and Inho Hwang*[,†]

[†]Department of Animal Science and BK21 PLUS Program and [‡]Department of Animal Biotechnology, Jeonbuk National University, Jeonju 561-756, Republic of Korea

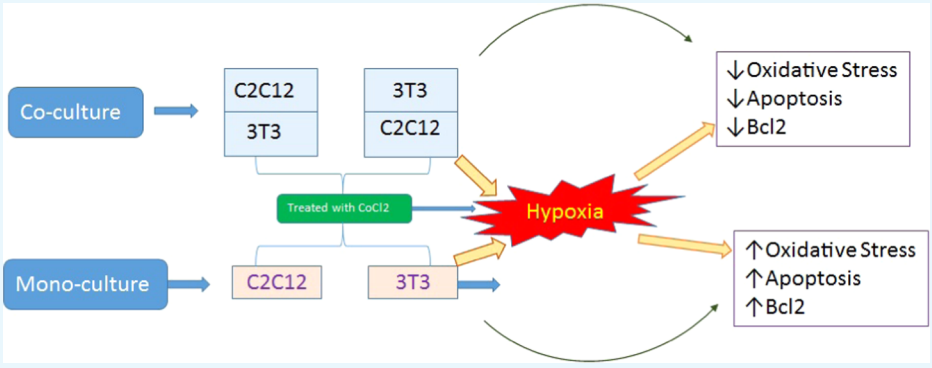

ABSTRACT: Cobalt chloride ($CoCl_2$) is a well-known hypoxia mimetic mediator that induces hypoxia-like responses. $CoCl_2$, a mediator confirmed to alleviate hypoxia-inducible factor-1 (HIF-1), has been associated with a variety of hypoxic responses. HIF-1 is the foremost transcriptionfactor that is particularly activated during hypoxia and regulates various genes. Therefore, this study aimed to investigate the cellular and molecular responses of the co-cultured cells under the influence of the $CoCl_2$-induced hypoxic condition. Mono- and co-cultured C2C12 and 3T3-L1 cells were exposed to $CoCl_2$, and a significant induction in HIF-1, reactive oxygen species and lipid peroxidase and a reduction in glutathione and catalase were observed. The expressions of proapoptotic genes like Bax, p53, caspase-9, and caspase-3 were notably increased, whereas the antiapoptotic gene, i.e., Bcl2, was downregulated during hypoxia in mono- as well as co-cultured C2C12 cells. However, the co-cultured C2C12 cells show significantly lower induction in oxidative stress and expression of apoptotic genes in comparison to monocultured C2C12 cells. Whereas, the co-cultured 3T3-L1 cells show comparatively higher oxidative stress and apoptotic event in comparison to monocultured 3T3-L1 cells. The reason may be the communication between the cells and some soluble factors that help in cell survival/death from hypoxia. Moreover, it may also be due to the fact that fat and muscle cells interact and communicate via proximity and mutual ability when growing together. Therefore, the co-culture system provides a unique approach to intercellular communication between the two different cell types.

INTRODUCTION

Mammalian cells have developed a unique feature of adaptation of survival under the hypoxic condition, and hypoxia controls the capability of a cell to sustain its energy level. To restore the oxygenation of the tissue, cells activate the expression of glycolytic genes[1] and start proliferation and angiogenesis. Due to severe hypoxia, the DNA mismatch repair activity of the cells is reduced, resulting in a high mutation rate.[2] Hypoxia also causes genetic variability via stimulation of fragile sites triggering gene amplification.[3,4] Therefore, cells start a cascade of the apoptotic event during severe hypoxia or anoxia conditions to prevent hypoxia-induced mutation in the cells.[5] Cobalt chloride ($CoCl_2$) is an eminent hypoxia imitative agent and finest chemical inducers of hypoxia-like responses.[6] Hypoxia-inducible factor-1 (HIF-1) is an imperative aspect of the hypoxia response, and it can induce apoptosis, stimulate cell proliferation, and prevent cell death.[7−9]

Several studies have shown that the introduction of $CoCl_2$ induces excessive construction of reactive oxygen species (ROS) and depolarization of the mitochondrial membrane by activating hypoxia-inducible factor-1α (HIF-1α) and several other mechanisms. In addition, it has also been shown that metal-induced ROS-mediated oxidative stress leads to commencement of nuclear transcription factors, a variety of signaling proteins, cell cycle arrest, and apoptosis[10] HIF-1α is unruffled of HIF-1α and ARNT subunits,[11] and it binds to the DNA motif of hypoxia response elements and is overexpressed during neovascularization. Nuclear factor kappa B has also been activated by hypoxia, which controls the transcription of many genes required for neovascularization, cells adhesion, differentiation, proliferation, and apoptosis.[12,13]

At the molecular level, hypoxia upregulates the hypoxia-inducible factor-1 (HIF-1) in muscle cells. The expressions of myoglobin, vascular endothelial growth factor, and glycolytic

Received: May 21, 2019
Accepted: November 13, 2019
Published: December 2, 2019

DOI: 10.1021/acsomega.9b01474
ACS Omega 2019, 4, 20882−20893

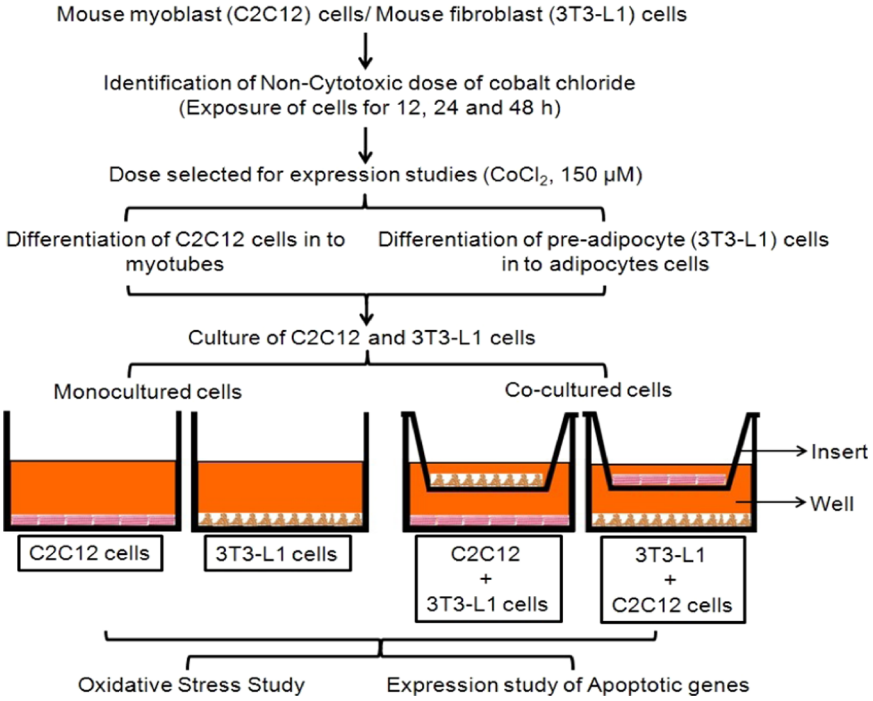

Figure 1. Experimental design.

enzymes were increased in a hypoxia-dependent approach after induction in the expression of HIF-1.[14,15] It has also been reported that the area of muscle structure and muscle fiber is changed during the severe hypoxia condition.[16] Moreover, cellular marks of mitochondrial humiliation stuff overcome under circumstances of augmented reactive oxygen species (ROS) formation.[17] Although an increase or decrease in ROS generation under the hypoxic condition is still controversial,[18] it seems that ROS could restrain the movement of HIF-1 and other redox-sensitive transcription factors.[19] Furthermore, ROS formation has also been revealed to exert hypoxia-induced cell death in various tissues through oxidative damage to macromolecules like nucleic acids, proteins, and membrane phospholipids.[20]

A growing body of evidence advocates that the $CoCl_2$-induced ROS production causes neuronal damage.[21−23] It is clearly shown that the high level of ROS attacks nucleic acids, proteins, and membrane phospholipids, which eventually lead to neuronal apoptosis.[24,25] Zou et al.[21] have reported that $CoCl_2$ stimulates cell death in PC12 cells via activating caspase-3 and p38 mitogen-activated protein kinase (MAPK). p38/MAPK is one of the apoptotic markers during PC12 cell death induced by a range of stimuli.[22,26] p38/MAPK, JNK, and ERK1/2, which are the members of MAPK family, have been activated by ROS formation in various cell types. Hypoxia/ischemia-induced neuronal cell death is associated with oxidative stress, which is responsible for neurogenerative disorders, like Parkinson's disease, Alzheimer's disease, and amyotrophic lateral sclerosis.[25,27] In the oxidative stress condition, ROS, superoxide (O_2^-), hydroxyl radical (HO^-), and H_2O_2 are produced in high amounts.[25,28] Oxidative stress induces too much amount of ROS that modifies the lipids, proteins, and DNA and alters their functions, causing apoptosis of neuronal cells.[29,30]

The co-culture system is the most powerful approach to study cell−cell communications and cell−cell interactions. Synthetic biologists use this system for studying and engineering complex multicellular synthetic systems. In the co-culture system, different cell types were cultured directly or indirectly within a similar culture environment. In straight co-cultures, cells are assorted collectively and allowed to make a direct contact within the same culture environment. In indirect co-cultures, cell interaction occurs via soluble factors within the culture environment and both the cell types are detached by the inserts.

To study the natural interactions between cell populations and to improve the culture success for certain populations, the co-culture system has been used. Moreover, the co-culture system provides an important platform for drug discovery because it offers a more illustrative in vivo-like model and helps in monitoring the effects of drugs on cell−cell interactions.[31] The co-culture system is also being used to overpass the fissure amid in vitro and in vivo model systems. The co-culture system has been used to learn immune defense and the effects of monocytes, eosinophils, neutrophils, and lymphocytes on epithelial cell function.[32] A few studies show that the co-culture system alters the messenger RNA (mRNA) expression of adipogenic marker genes in adipocytes. For instance, the adipogenic marker genes of differentiated 3T3-L1 cells have been upregulated by C2C12 cells when both the cells were co-cultured.[33] The expression of C/EBPb and GPR43 genes increased in adipocytes when the bovine muscle satellite cells were co-cultured with preadipocytes.[34] In addition, the differentiation of porcine preadipocytes was repressed in the co-culture system and the expression of marker genes in the previous phase of adipogenic differentiation was lesser than that in the monocultured cells.[35]

In fetal, postnatal, and adult animals, the muscle development process starts earlier than the fat cells. The budding fat cells, near to muscles, go through all development and differentiation phases in secure immediacy alike mature, multinucleated, and functional skeletal muscles.[36] The intend

DOI: 10.1021/acsomega.9b01474
ACS Omega 2019, 4, 20882−20893

of the current study was to explore the impact of $CoCl_2$ exposure on the modulation of a variety of genes associated with hypoxia such as HIF-1α and apoptosis such as Box, Bcl2, p53, and caspase-9/3 in the co-culture system.

MATERIALS AND METHODS

Reagents and Consumables. The specified chemicals, reagents, and the culture medium were purchased from Sigma-Aldrich (St. Louis, MO) and Gibco BRL. All of the culture wares were procured from Nunc, Denmark, for the study. Throughout the study, Milli-Q water was used.

Cell Culture. The C2C12 (mouse myoblast) and 3T3-L1 (mouse preadipocyte) cell lines were ordered from American Type Culture Collection (Manassas), and both cell lines were cultured and maintained as the method given by the provider at the Department of Animal Science and Biotechnology, Jeonbuk National University, Jeonju, Republic of Korea. In brief, the specific culture medium [Dulbecco's modified Eagle's medium (DMEM), 10% fetal bovine serum (FBS), 0.2% sodium bicarbonate, and 1% antibiotic] was used to culture the C2C12 and 3T3-L1 cell lines and kept in a CO_2 incubator having 37 °C temperature, 5% CO_2, and 95% humidity. Once the confluency reached up to 75−85%, we pass the culture in 1:6 ratio and change the medium two times in a week. Mycoplasma contamination was not found throughout the study. The trypan blue dye exclusion assay was used to check the cell viability before starting all of the experiments, and the culture having 95% or more cell viability was used.

EXPERIMENTAL DESIGN

A diagramatic representation of the experimental design is shown in Figure 1.

Cytotoxicity Assessment [3-(4,5-Dimethylthiazol-2-yl)-2,5-diphenyltetrazolium Bromide (MTT) Assay]. The MTT assay was used to measure the cytotoxicity by using the method described by Kumar.[37] In brief, 96-well plates were used to culture the C2C12 and 3T3-L1 cells and 1×10^4 cells were seeded in each well. The culture plates were kept for 24 h in a CO_2 incubator, and after 24 h, the medium was removed and the cells were exposed with $CoCl_2$ (37.5, 75, 150, and 300 μM) for 12−48 h in the CO_2 incubator. MTT salt (10 μL, 5 mg/mL stock solution) was added in each well 4 h before reaching their respective time periods. After completion of their respective time periods, the medium containing $CoCl_2$ and MTT salt was removed and 200 μL of dimethyl sulfoxide per well was used to dissolve the formazan crystals. The plates were kept for 10 min at room temperature, and a multiwell microplate reader was used to obtain absorbance at 550 nm (Synergy HT, Bio-Tek). Correspondingly, the control sets were also run without exposure to $CoCl_2$ in the same environment.

Differentiation of Preadipocyte (3T3-L1) to Adipocyte Cells. The DMEM (contains 10% FBS and 1% penicillin/streptomycin) was used to culture the 3T3-L1 cells, and the culture plates were kept in the CO_2 incubator and maintained as described earlier. The differentiation medium [differentiation medium composition: 90% Dulbecco's modified Eagle's medium (DMEM), 10% fetal bovine serum (FBS), 0.5 mM methylisobutylxanthine, 1.0 μM dexamethasone, 2.0 μM rosiglitazone, and 1.0 μg/mL insulin] was used to differentiate the preadipocytes into adipocytes. The adipocytes were maintained in adipocyte maintenance medium (90% Dulbecco's modified Eagle's medium, 10% fetal bovine serum, and 1.0 μg/mL insulin). In brief, the 70−80% confluent 3T3-L1 cells were harvested by trypsinization and seeded in a six-well culture plate supplemented with complete DMEM for 48 h or more to achieve 100% confluence. The cells were incubated in differentiation medium for 48 h, and after that, the medium was changed with adipocyte maintenance medium. The adipocyte maintenance medium was changed every 48−72 h. The preadipocytes will take 7−15 days after the induction to differentiate into fully mature adipocytes, which can be seen by lipid droplet formation.

Oil Red O Cell Staining. The oil red O (0.35 g) dye was procured from Sigma-Aldrich. The dye was dissolved in isopropanol (100 mL) and kept for 12−14 h at room temperature. The Whatman filter paper was used to remove the precipitate formed in the solution. The working solution (0.1%) was prepared by mixing 30 mL of water into 60 mL of filtered dye solution and kept for 12−14 h at 4 °C. The solution was filtered two times before staining the cells. The cells were washed two times with phosphate-buffered saline (PBS) and fixed for 1 h in 4% paraformaldehyde. After 1 h, the cells were washed again two to three times with PBS, and 0.1% oil red O working solution was added into the plates for 1−2 h. After completion of the incubation period, the cells were washed three times with PBS and the images of the cells were captured by a phase contrast microscope.

Differentiation of C2C12 Cells to Myotubes. C2C12 mouse myoblasts were cultured in DMEM and maintained in a CO_2 incubator, and the cell viability was determined with the help of the trypan blue dye exclusion assay. Prior to the start of differentiation, the DMEM having 10% fetal bovine serum was replaced with 1% fetal calf serum[38] to induce the differentiation of myoblasts into myotubes.

Co-culture of C2C12 and 3T3-L1. Transwell inserts having a 0.4 μm porous membrane were used to co-culture C2C12 and 3T3-L1 according to the protocol of Sun.[39] C2C12 and 3T3-L1 cells were cultured separately on the transwell plates. Once the cells differentiated, the inserts having 3T3-L1 were transferred to the C2C12 cell plate and vice versa. The cells were allowed to grow together for 12, 24, and 48 h; after that, the cells present in the lower wells of the insert were harvested for further study.

Cell Viability by the Trypan Blue Dye Exclusion Assay. Cell viability was determined by using the trypan blue dye exclusion assay in which the loss of membrane integrity was assessed.[40] In brief, 1×10^5 cells per well were seeded in six-well culture plates and kept for 24 h in a CO_2 incubator to grow properly. Then, the normal DMEM was changed with the medium containing $CoCl_2$ (37.5, 75, and 150 μM) for 12, 24, and 48 h. Following the exposure, the cells were subjected to measure the cell viability. After the completion of the respective time periods, the cells were harvested, centrifuged at 800 rpm for 5 min, washed two times with sterile PBS, and resuspended in a small amount of PBS. The trypan blue dye (0.4% solution) was mixed with cell suspension in a 1:5 ratio (dye/cell suspension). The cell suspension solution (10 μL) with trypan blue was put on a hemocytometer, and unstained live and blue-stained dead cells were counted under a phase contrast microscope. The control sets without exposure to $CoCl_2$ were also run in the same environment.

MTT Assay of Co-cultured Cells. The MTT assay of co-cultured cells has been carried out by using the same method as described in the previous section.

DOI: 10.1021/acsomega.9b01474
ACS Omega 2019, 4, 20882−20893

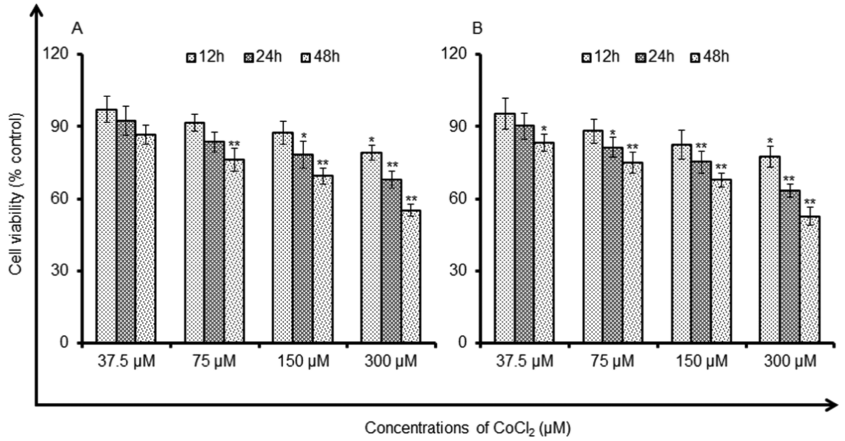

Figure 2. Identification of noncytotoxic dose of cobalt chloride ($CoCl_2$) in C2C12 and 3T3-L1 cells. The cells were exposed to $CoCl_2$ (37.5−300 μM) for 12−48 h in C2C12 (A) and 3T3-L1 cells (B). The percent cell viability was assessed using the MTT assay. Values are given as mean ± standard error of the data obtained from three independent experiments. *$p < 0.05$, **$p < 0.01$.

Reactive Oxygen Species (ROS) Generation. 2′,7′-Dichlorodihydrofluorescein diacetate (DCFH-DA; Sigma-Aldrich) fluorescent dye[41] has been used to measure the ROS generation induced by hypoxia in both mono- and co-cultured cells. In brief, six-well plates were used to culture the C2C12 and 3T3-L1 cells (1×10^5 cells/well) and allowed to remain for 24 h in a CO_2 incubator. Both the mono- and co-cultured cells were exposed with $CoCl_2$ (150 μM) for 12, 24, and 48 h. The DCFH-DA (20 μM) dye was added into the cells for 30 min at 37 °C after the completion of the respective time periods. The cells containing culture medium and DCFH-DA dye were changed with 200 μL of PBS per well, and the plates were shaken for 10 min at room temperature in the dark condition The fluorescence strength was calculated by using a multiwell microplate reader (Synergy HT, Bio-Tek) at 485 and 528 nm of excitation and emission wavelengths, respectively. The unexposed cells were also run, and the data were presented as a percentage of control.

Glutathione (GSH) Content Measurement. The glutathione content was assessed by using the method of Vivek et al.[42] The mono- and co-cultured cells receiving exposure of $CoCl_2$ (150 μM for 12, 24, and 48 h) were washed two times with cold PBS. The deoxycholic acid with sucrose solution was added to prepare the cell lysate and centrifuged at 10 000*g* for 10 min at 4 °C. Perchloric acid (1%) was taken to precipitate the protein present in the supernatant solution and further centrifuged at 10 000*g* for 5 min at 4 °C. The precipitated protein (20 μL) was taken in a 96-well black bottom plate and mixed with 160 μL of 0.1 M phosphate, 5 mM ethylenediaminetetraacetic acid (EDTA) buffer (pH 8.3), and 20 μL of *o*-phthalaldehyde (1 mg dissolved in 1 mL of methanol). The plates were kept for 3 h in a dark place at room temperature for incubation, and then, fluorescence was recorded at 355 and 460 nm of excitation and emission wavelengths, respectively, with the help of a multiwell microplate reader (Synergy HT, Bio-Tek). Perchloric acid (1%) was used as a standard of GSH, and the results were presented in nanomoles of GSH/mg cellular protein.

Lipid Peroxidation (LPO). The thiobarbituric acid (TBA)-reactive substance protocol[43] was used to measure lipid peroxidation. In brief, both the C2C12 and 3T3-L1 cells were cultured and 1×10^5 cells/well were sown in six-well plates for 24 h in the CO_2 incubator. The 150 μM concentration of $CoCl_2$ was used to treat both the cells for 12, 24, and 48 h. The cells present in lower wells were harvested once they reached to their respective time periods. The cells were sonicated in chilled 1.15% potassium chloride solution at 3000*g* for 10 min to collect the supernatant. The thiobarbituric acid reagent (2 mL; composition: 0.7% TBA, 15% trichloroacetic acid, and 0.25 N HCl) was mixed with 1 mL of supernatant, and the mixture was kept in a water bath for 15 min at 100 °C. Finally, the mixture was centrifuged for 10 min at 1000*g* and the 535 nm wavelength was used to calculate the absorbance of the supernatant. All of the values are represented as a percentage of control.

Assessment of Catalase Levels. The assessment of catalase activity was done with the help of a commercially accessible kit (Catalog no. 707002; Cayman Chemicals) and the instructions given by the manufacturer. In concise, C2C12 and 3T3-L1 cells (1×10^5 cells/well) were seeded in six-well plates in a CO_2 incubator for 24 h to normalize. Both the mono- and co-cultured cells were treated with $CoCl_2$ (150 μM) for 12, 24, and 48 h. Once the time periods over, the cells were harvested and centrifuged at 1000*g* for 10 min at 4 °C to obtain the cell pellet. The cells were sonicated in chilled buffer (1.0 mL) having the composition 50 mM potassium phosphate, pH 7.0, and 1 mM EDTA. The supernatant was collected for analysis by centrifugation at 10 000*g* for 15 min at 4 °C. Furthermore, the reaction was started by adding 20 μL of 0.88 M hydrogen peroxide in the reaction mixture containing 20 μL of sample, 100 μL of assay buffer (provided in the kit), and 30 μL of methanol in a 96-well plate. The plate was kept for incubation on a shaker at room temperature, and after 20 min, potassium hydroxide (30 μL) was added to stop the reaction. Afterward, 30 μL of chromogen was supplemented and incubated for 10 min accompanied by adding 10 μL of potassium periodate. The plates were set aside for 5 min at room temperature, and the absorbance was recorded at 540 nm with the help of a multiwell microplate reader (Synergy HT, Bio-Tek).

Transcriptional Changes. Hypoxia-induced alterations in the RNA level of genes involved in apoptosis such as Bax, Bcl2, p53, caspase-3, and caspase-9 were studied in both mono- and co-cultured cells by using the protocol of Kumar.[44] Hypoxia-induced alterations in the mRNA level were articulated in fold change with respect to control cells. In short, total RNA from

DOI: 10.1021/acsomega.9b01474
ACS Omega 2019, 4, 20882−20893

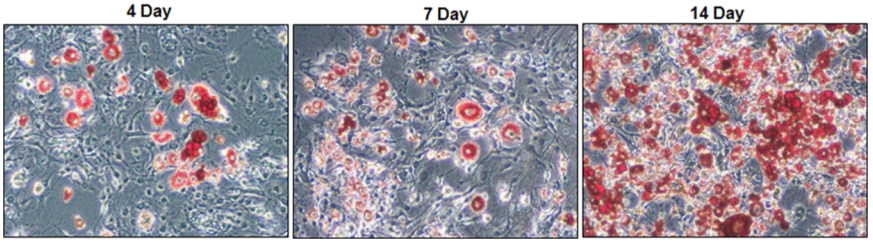

Figure 3. Differentiation of preadipocyte cells (3T3-L1) to adipocyte cells. After co-culturing, 3T3-L1 preadipocytes were induced to differentiation, the inverted microscope images on days 4, 7, and (Oil Red O-stained) were shown, and the cell triglyceride accumulation was detected.

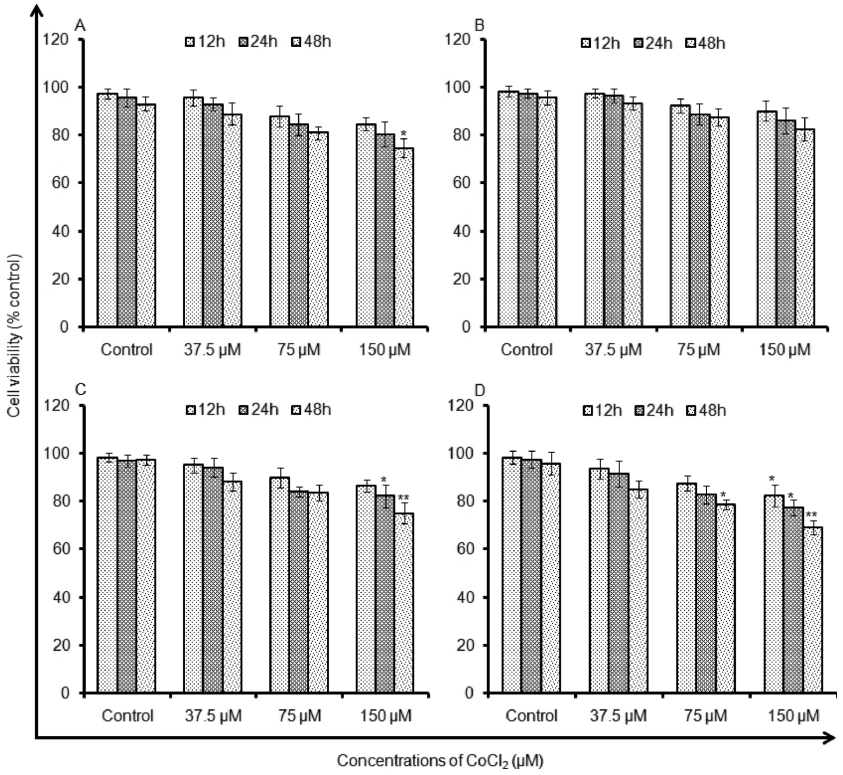

Figure 4. Cytotoxicity assessment of cobalt chloride ($CoCl_2$) in mono- and co-cultured C2C12 and 3T3-L1 cells (trypan blue dye exclusion assay). Monoculture C2C12 cells (A), co-cultured C2C12 cells (B), monocultured 3T3-L1 cells (C), and co-cultured 3T3-L1 cells (D) were exposed to $CoCl_2$ (37.5−150 μM) for 12−48 h. The data presented are percent cell viability compared to unexposed control cells. Values are given as mean ± standard error of the data obtained from three independent experiments. *$p < 0.05$, **$p < 0.01$.

treated and control cells was isolated with the help of the TRI reagent (Catalog no. T9424, Sigma-Aldrich). Complementary DNA (cDNA) was prepared by 1 μg of RNA with the help of a High Capacity cDNA Reverse Transcription Kit (Catalog no. 4368814, Applied Biosystems), and 2× SYBR Green polymerase chain reaction (PCR) master mix (Applied Biosystems) was used for real-time PCR in a Bio-Rad Sequence Detection System. For every sample, three reactions were done in three different wells and β-actin was used as an internal control.

Statistical Analysis. The values in results are articulated as mean ± standard error (SE) of three autonomous experiments. To identify the differences among treated and control groups, one-way analysis of variance pursued by post hoc Dunnett's test was used. *$p < 0.05$ was used to designate the significant changes.

RESULTS

Cytotoxicity Assessment (MTT Assay). The results of the MTT assay are shown in Figure 2. C2C12 and 3T3-L1 cells responded to $CoCl_2$ in a dose- and time-dependent manner. There was no significant reduction in percent cell viability till 24 h after exposure to 37.5 μM concentration of $CoCl_2$, whereas the concentrations of $CoCl_2$ used, i.e., 150 and 300 μM, were found to cause a more steady reduction in percent cell viability, which reached significant levels at and above the exposure period of 24 h. The cell viability reduces to 87.49 ± 4.69, 78.36 ± 5.63, and 69.52 ± 3.35 at 12, 24, and 48 h, respectively, after exposure to 150 μM $CoCl_2$ in C2C12 cells. The reduction was more in C2C12 cells when they were exposed to the highest concentration, i.e., 300 μM, where the viability reduces to 79.23 ± 3.22, 67.94 ± 3.71, and 55.17 ± 2.53 at 12, 24, and 48 h, respectively, compared to unexposed control cells (Figure 2A). Trends were similar in the case of 3T3-L1 cells, which show 82.47 ± 6.11, 75.33 ± 4.53, and

DOI: 10.1021/acsomega.9b01474
ACS Omega 2019, 4, 20882−20893

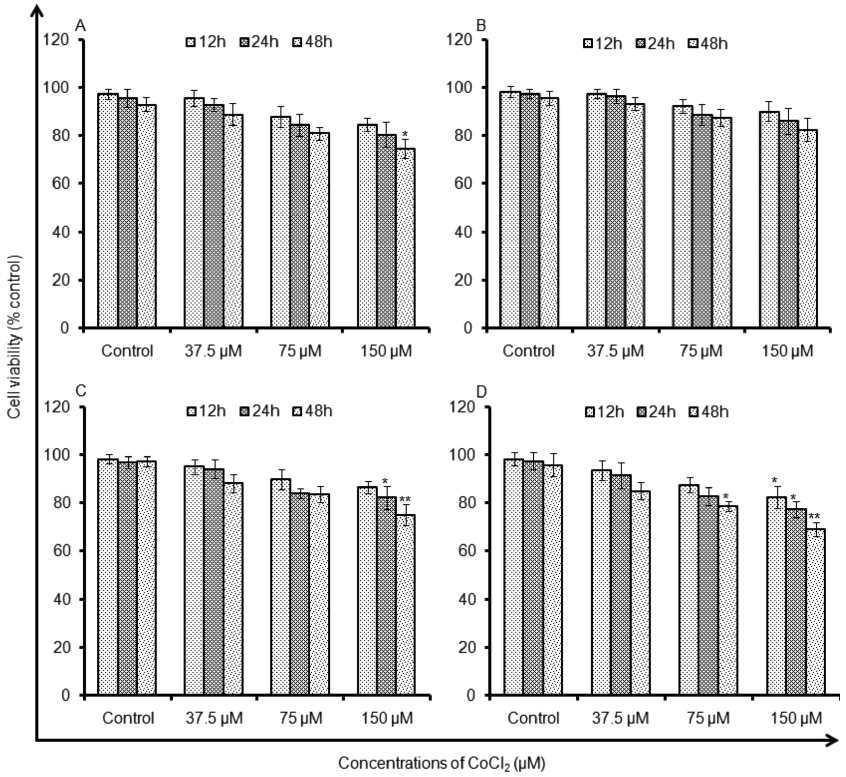

Figure 5. (A–D) Cytotoxicity assessment of cobalt chloride ($CoCl_2$) in mono- and co-cultured C2C12 and 3T3-L1 cells (MTT assay). The monocultured and co-cultured cells were exposed to $CoCl_2$ (150 μM) for 12–48 h. The data presented are percent cell viability compared to unexposed control cells. Values are given as mean ± standard error of the data obtained from three independent experiments. *p < 0.05, **p < 0.01.

67.88 ± 2.86 reduction in cell viability when exposed to 150 μM and it reached its peak, i.e., 77.51 ± 4.43, 63.48 ± 2.73, and 52.77 ± 3.61 after exposure to 300 μM $CoCl_2$ for periods of 12, 24, and 48 h, respectively, compared to unexposed control cells (Figure 2B).

Differentiation of Preadipocyte (3T3-L1) to Adipocyte Cells. The 3T3-L1 cells were cultured in complete DMEM for 24 h at 37 °C, 5% CO_2, and 95% humidity atmosphere conditions. Then, the medium was completely changed to differentiated medium and the cells were left for differentiation for 48 h. After 48 h, the adipocytes were kept in adipocyte maintenance medium in place of differentiation medium and changed every 48–72 h. The preadipocyte cells were completely differentiated into adipocytes between 7 and 15 days following induction, as shown by lipid droplet structures in Oil Red O staining (Figure 3).

Trypan Blue Dye Exclusion Assay. The straight loss in the viable cell count was also assessed instantly after exposure to $CoCl_2$ at each time point (12, 24, and 48 h) using the trypan blue dye exclusion test. The result highlights are shown in Figure 4. At 48 h, a statistically significant drop in the percent cell viability was found and it sustained in all time periods (24 and 48 h) after exposure to 37.5, 75, and 150 μM concentrations of $CoCl_2$. At 24 h, the co-cultured C2C12 cells show 96.58 ± 2.95, 88.99 ± 4.22, and 86.27 ± 5.46% cell viability and 93.39 ± 2.73, 87.62 ± 3.56, and 82.55 ± 4.83% cell viability at 48 h after the exposure to 37.5, 75, and 150 μM concentrations of $CoCl_2$ (Figure 4A). However, the monocultured C2C12 cells show the reduction in cell viability, i.e., 93.04 ± 2.58, 84.61 ± 4.47, and 80.64 ± 5.27% at 24 h and 88.99 ± 4.57, 81.18 ± 2.67, and 74.72 ± 3.93% at 48 h after exposure to 37.5, 75, and 150 μM concentrations of $CoCl_2$ (Figure 4B).

Similarly, the co-cultured 3T3-L1 cells show 91.73 ± 5.50, 83.03 ± 3.75, and 77.45 ± 3.28% at 24 h and 85.21 ± 3.54, 78.84 ± 1.97, and 69.14 ± 3.02% cell viability at 48 h after exposure to 37.5, 75, and 150 μM concentrations of $CoCl_2$, respectively (Figure 4C). However, the monocultured 3T3-L1 cells show a significant reduction in cell viability, i.e., 94.30 ± 3.84, 84.11 ± 2.20, and 82.47 ± 4.76% at 24 h and 88.23 ± 3.78, 83.80 ± 3.34, and 75.26 ± 4.42% at 48 h after exposure to 37.5, 75, and 150 μM concentrations of $CoCl_2$, respectively (Figure 4D).

MTT Assay of Co-cultured Cells. The results of the MTT assay of co-cultured cells are shown in Figure 5. There was a reduction in percent cell viability throughout the exposure periods, i.e., till 48 h in the co-cultured cells after exposure to 150 μM $CoCl_2$. However, the 150 μM concentration of $CoCl_2$ was responsible for more diminution in percent cell viability of monocultured C2C12 cells, which reaches to a significant stage at and over the exposure period of 24 h. The cell viability reduces to 96.59 ± 5.33, 92.34 ± 4.02, and 88.21 ± 4.69% at 12, 24, and 48 h, respectively, after exposure to 150 μM $CoCl_2$ in co-cultured C2C12 cells. The reduction was more pronounced in monocultured C2C12 cells exposed to 150 μM concentration of $CoCl_2$, where the cell viability reduces to 91.38 ± 4.16, 83.62 ± 3.38, and 75.44 ± 4.92%. However, the co-cultured 3T3-L1 cells show 87.44 ± 8.91, 79.26 ± 6.13, and 69.73 ± 4.69% and the monocultured 3T3-L1 cells show 90.15 ± 4.42, 84.51 ± 5.61, and 77.69 ± 3.98% cell viability after exposure to 150 μM $CoCl_2$ for periods of 12, 24, and 48 h, respectively, compared to unexposed control cells. The

DOI: 10.1021/acsomega.9b01474
ACS Omega 2019, 4, 20882–20893

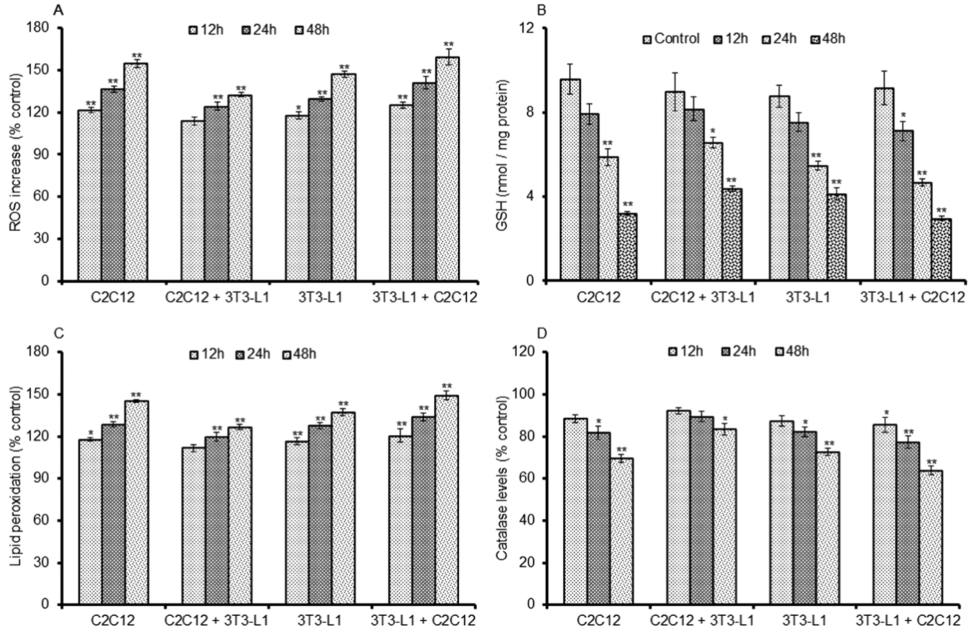

Figure 6. Oxidative stress study in mono- and co-cultured C2C12 and 3T3-L1 cells. Percent change in ROS generation (a), GSH activity (b), change in levels of lipid peroxidation (c), and catalase activity (d) after exposure to 150 μM concentration of $CoCl_2$ for 12, 24, and 48 h time periods assessed by the microplate reader. Data represented are the mean ± standard error of three identical experiments made in three replicates. *$p < 0.05$ and **$p < 0.01$ in comparison to respective unexposed controls.

reduction in cell viability was more in co-cultured 3T3-L1 cells in comparison to monocultured 3T3-L1 cells (Figure 5).

Reactive Oxygen Species (ROS) Generation. The results of $CoCl_2$-induced ROS formation are shown in Figure 6A. Monocultured C2C12 cells show significant ($p < 0.01$) receptiveness against $CoCl_2$ (150 μM) at all time points and show 121.64 ± 3.76, 136.42 ± 4.77, and 154.73 ± 2.47% ROS generation at 12, 24, and 24 h, respectively. However, the induction of ROS generation was comparatively reduced in co-cultured in comparison to monocultured C2C12 cells. The co-cultured C2C12 cells show the significant decrease in ROS generation, i.e.,113.86 ± 3.10, 124.26 ± 5.27, and 132.55 ± 4.28% after exposure to $CoCl_2$ (150 μM) for 12, 24, and 48 h, respectively, in comparison to unexposed control cells. At the same time, ROS generation was also studied in monocultured 3T3-L1 cells that show 117.92 ± 4.69, 129.66 ± 2.78, and 147.28 ± 3.58%; however, co-cultured 3T3-L1 cells show significantly higher ROS generation, i.e.,125.38 ± 2.22, 141.18 ± 4.40, and 159.52 ± 5.50% in comparison to monocultured cells at 12, 24, and 48 h of $CoCl_2$ (150 μM) exposures.

Glutathione Content Measurement. Cells exposed to $CoCl_2$ (150 μM) were found to show a decrease in the level of GSH notably at all of the time points in monocultured C2C12 cells, in comparison to control. While the co-cultured C2C12 cells could not cause such rigorous effects, the trends were similar. The co-cultured C2C12 cells show the least toxicity in comparison to monocultured C2C12 cells. However, the monocultured 3T3-L1 cells show a higher decrease in the level of GSH in comparison to co-cultured 3T3-L1 cells (Figure 6B).

Lipid Peroxidation (LPO). $CoCl_2$ (150 μM) induced significant lipid peroxidation in monocultured C2C12 cells at exposure times of 12 h (117.92 ± 3.01%), 24 h (128.37 ± 5.58%), and 48 h (145.24 ± 3.59%) in comparison to that in control. The trends were similar in the case of co-cultured C2C12 cells, but the induction of lipid peroxidation was less in comparison to monocultured C2C12 cells. The co-cultured C2C12 cells show 111.77 ± 2.55, 119.68 ± 4.23, and 126.44 ± 4.69% LPO at 12, 24, and 48 h, respectively, after exposure to 150 μM $CoCl_2$ in comparison to unexposed control cells (Figure 6C). The monocultured 3T3-L1 cells show 116.68 ± 2.04, 127.59 ± 3.15, and 137.46 ± 4.13%, while the co-cultured 3T3-L1 cells show 120.55 ± 8.10, 133.82 ± 4.90, and 149.35 ± 5.24% LPO at 12, 24, and 48 h, respectively, in comparison to unexposed control cells (Figure 6C).

Assessment of Catalase Level. A significant decline in the catalase activity was ascertained at 150 μM $CoCl_2$, and the monocultured C2C12 cells show 88.39 ± 5.38, 81.67 ± 4.42, and 69.54 ± 3.67% catalase activity at 12, 24, and 48 h, respectively. The trends were also similar in the case of co-cultured C2C12 cells which show 92.15 ± 3.52, 89.33 ± 2.52, and 83.48 ± 4.51% catalase activity at 12, 24, and 48 h, respectively (Figure 6D). However, the monocultured 3T3-L1 cells show 87.28 ± 3.24, 82.12 ± 4.80, and 72.63 ± 2.72% catalase activity, while the co-cultured 3T3-L1 cells show 85.52 ± 3.59, 77.29 ± 3.01, and 63.94 ± 2.16 at 12, 24, and 48 h, respectively, in comparison to unexposed control cells (Figure 6D).

Transcriptional Changes in Genes Associated with Hypoxia and Apoptosis. Alteration in the RNA level of the genes involved in hypoxia and apoptosis was studied in both monocultured and co-cultured cells following the introduction of $CoCl_2$ (150 μM). The significant upregulation of hypoxia-inducible factor (HIF-1α) and proapoptotic genes such as Bax, p53, caspase-3, and caspase-9 and the downregulation of an antiapoptotic gene such as Bcl2 have been recorded following treatment with 150 μM $CoCl_2$ in both mono- and co-cultured cells. The expression of HIF-1α increases significantly from 6.89 ± 0.32- to 14.24 ± 0.45-fold in monocultured C2C12 cells and 5.89 ± 0.19- to 12.46 ± 0.43-fold in co-cultured C2C12 cells at 12−48 h, respectively, after exposure to $CoCl_2$. The monocultured C2C12 cells showed more apoptotic

DOI: 10.1021/acsomega.9b01474
ACS Omega 2019, 4, 20882−20893

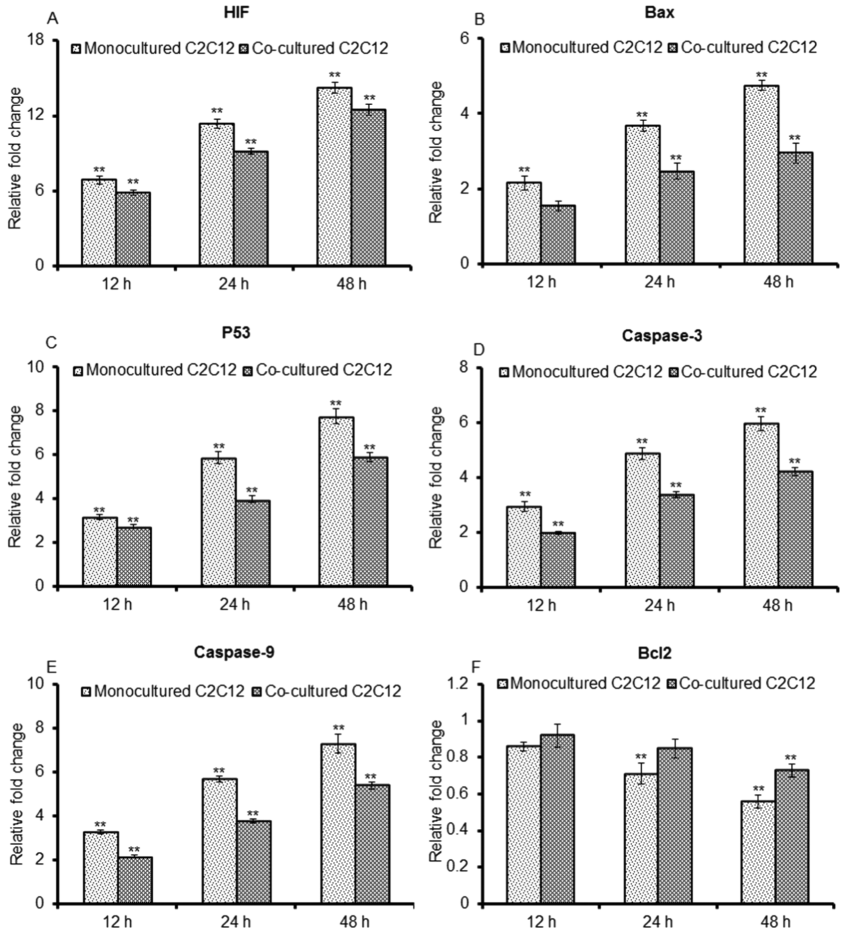

Figure 7. (A–F) Real-time PCR analysis for transcriptional changes in apoptotic genes in monocultured and co-cultured C2C12 cells. Fold changes in altered mRNA expression of apoptotic genes in monocultured and co-cultured C2C12 cells following the exposure to $CoCl_2$ (12–48 h). β-Actin was used as an endogenous control to normalize the data, and $CoCl_2$-induced alterations in transcripts were expressed in fold changes (mean ± standard error) compared to unexposed controls. *$p < 0.05$ and **$p < 0.01$ in comparison to respective unexposed controls.

response in comparison to co-cultured C2C12 cells after exposure to $CoCl_2$ (150 μM). The monocultured C2C12 cells show the upregulation of Bax (2.15 ± 0.18, 3.68 ± 0.16, and 4.76 ± 0.12 fold), p53 (3.12 ± 0.12, 5.85 ± 0.27, and 7.74 ± 0.34 fold), caspase-3 (2.94 ± 0.19, 4.87 ± 0.22, and 5.96 ± 0.24 fold), and caspase-9 (3.27 ± 0.09, 5.68 ± 0.14, and 7.29 ± 0.43 fold) and the downregulation of Bcl2 (0.86 ± 0.02, 0.71 ± 0.06, and 0.56 ± 0.03 fold) at the contact periods of 12, 24, and 48 h correspondingly after exposure to $CoCl_2$ (Figure 7). The trends were similar in the expression of pro- and antiapoptotic genes in co-cultured C2C12 cells; however, the 3T3-L1 cells protect the C2C12 cells from apoptosis after exposure to $CoCl_2$ and show the expression of Bax (1.54 ± 0.13, 2.46 ± 0.21, and 2.95 ± 0.26 fold), p53 (2.72 ± 0.08, 3.96 ± 0.16, and 5.89 ± 0.20 fold), caspase-3 (1.98 ± 0.06, 3.38 ± 0.10, and 4.21 ± 0.14 fold), and caspase-9 (2.15 ± 0.07, 3.77 ± 0.10, and 5.39 ± 0.17 fold) and downregulation of Bcl2 (0.92 ± 0.06, 0.85 ± 0.05, and 0.73 ± 0.03 fold) at the same time points (Figure 7).

The monocultured 3T3-L1 cells show the expression of HIF-1α 7.91 ± 0.14, 10.15 ± 0.21, and 15.23 ± 0.44 fold and co-cultured 3T3-L1 cells show 8.64 ± 0.20, 10.49 ± 0.30, and 16.45 ± 0.34 fold at 12, 24, and 48 h, respectively, after exposure to $CoCl_2$. The monocultured 3T3-L1 cells show the upregulation of Bax (2.36 ± 0.10, 3.79 ± 0.07, and 4.25 ± 0.18 fold), p53 (2.87 ± 0.30, 4.49 ± 0.18, and 5.67 ± 0.24 fold), caspase-3 (3.83 ± 0.27, 4.86 ± 0.20, and 5.69 ± 0.24 fold), and caspase-9 (3.97 ± 0.13, 6.08 ± 0.23, and 7.13 ± 0.28 fold) and the downregulation of Bcl2 (0.81 ± 0.03, 0.74 ± 0.04, and 0.68 ± 0.02 fold) at the contact periods of 12, 24, and 48 h in that order after exposure to $CoCl_2$ (Figure 8). The tendencies were similar in the expression of pro- and antiapoptotic genes in co-cultured 3T3-L1 cells; however, the expression of apoptotic genes increased after exposure to $CoCl_2$ and it shows the expression of Bax (2.93 ± 0.10, 4.37 ± 0.22, and 5.78 ± 0.17 fold), p53 (3.61 ± 0.17, 5.25 ± 0.12, and 6.94 ± 0.21 fold), caspase-3 (4.47 ± 0.15, 5.98 ± 0.11, and 6.85 ± 0.30 fold), and caspase-9 (4.85 ± 0.21, 7.39 ± 0.31, and 8.67 ± 0.36 fold) and the downregulation of Bcl2 (0.76 ± 0.07, 0.67 ± 0.08, and 0.59 ± 0.03 fold) at the same time points (Figure 8). The mono- and co-cultured cells were compared to control cells, and we found that they are statistically significant. After that, we compared the mono- and co-cultured cells with each other and found that they are statically significant for all of the apoptotic genes.

DISCUSSION

The arrangement of cellular processes has been affected by the decrease in the level of oxygen, which is the most causative aspect in several pathologies.[45,46] In hypoxia, ROS modulate the expression of genes concerned in signal transduction.[47] Oxidative stress results due to constant hypoxia and excessive

DOI: 10.1021/acsomega.9b01474
ACS Omega 2019, 4, 20882–20893

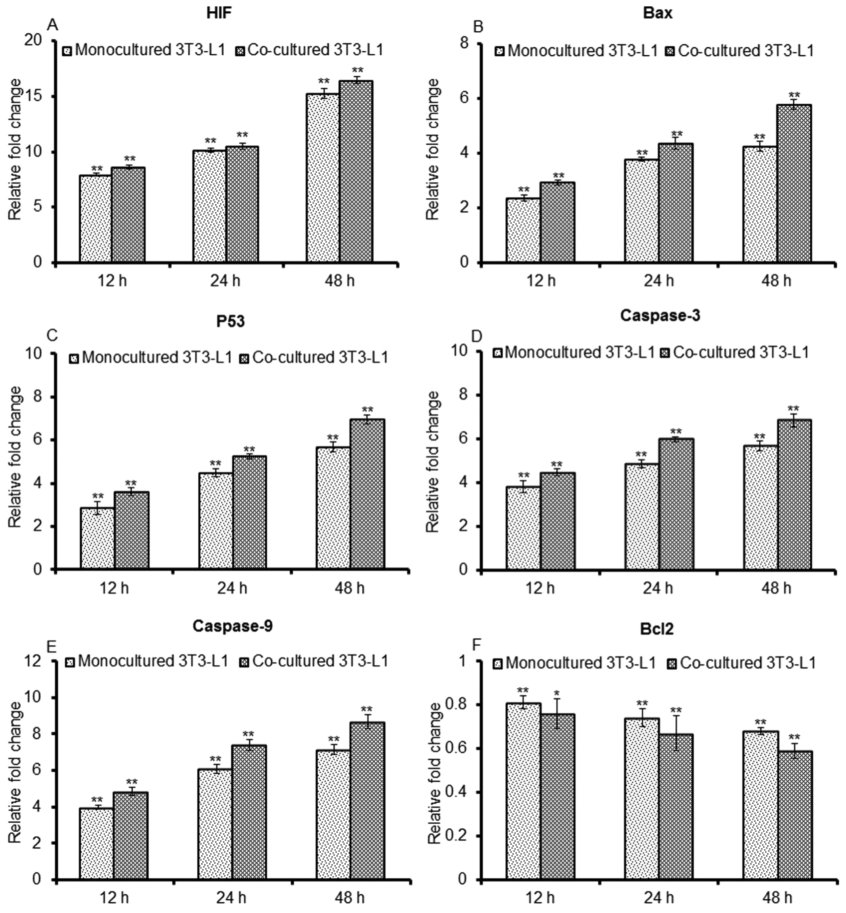

Figure 8. (A–F) Real-time PCR analysis for transcriptional changes in apoptotic genes in monocultured and co-cultured 3T3-L1 cells. Fold changes in altered mRNA expression of apoptotic genes in monocultured and co-cultured 3T3-L1 cells following exposure to $CoCl_2$ (12–48 h). β-Actin was used as an endogenous control to normalize the data, and $CoCl_2$-induced alterations in transcripts were expressed in fold changes (mean ± standard error) compared to unexposed controls. *$p < 0.05$ and **$p < 0.01$ in comparison to respective unexposed controls.

ROS production, which may be concomitant in the induction of apoptosis.[48] Cobalt chloride mimics the hypoxia-like response by upregulating the genes and promoting cell death in many cellular systems. We exposed the cells with $CoCl_2$ to study the molecular and cellular responses of both mono- and co-cultured cells toward hypoxia and the potential involvement of free radicals in reaction to hypoxia.

In this study, we found that the exposure to nontoxic concentration of $CoCl_2$ triggers the activation of HIF-1α, oxidative stress, and apoptotic cell death in both mono- and co-cultured cells. ROS formation was significantly induced in both mono- and co-cultured C2C12 and 3T3-L1 cells after exposure to $CoCl_2$. However, the level of ROS generation was lower in co-cultured C2C12 cells in comparison to monocultured C2C12 cells. On the other hand, the 3T3-L1 co-cultured cells showed more ROS generation in comparison to monocultured 3T3-L1 cells. An enhancement in intracellular ROS has been reported in different cell types after exposure to $CoCl_2$.[23,49] It has been previously noted in diverse cell types that ROS formation acts directly on the mitochondria and accelerates the loss of mitochondrial membrane potential. However, the signaling pathway remains provocative and there is some contradiction regarding $CoCl_2$, which can stimulate both the intrinsic[23] and extrinsic[50,51] apoptosis pathways. There are some reports showing that the ROS formation increases during the hypoxia condition,[52,53] while others show a decrease.[54,55] During hypoxia, the expression of HIF-1 was found to be increased, which regulates the mitochondrial activity,[56] and precisely ROS formation.[18,53,57] However, few studies also showed an increase in ROS generation with a reduction in the expression of HIF-1.[58,59]

GSH forms within the cells having thiol groups and is affected by $CoCl_2$ exposure.[60] GSH maintains the redox homeostasis by protecting the cells from oxidative damage. However, we detected the depletion of GSH in both mono- and co-cultured cells receiving exposure of $CoCl_2$, but the enormity of diminution was statistically larger in the monocultured C2C12 cells in comparison to co-cultured C2C12 cells. The monocultured 3T3-L1 cells have less depletion in the level of GSH in comparison to co-cultured 3T3-L1 cells. Thus, the depletion of GSH levels in both mono- and co-cultured cells could be accredited to the enlarged consumption of GSH-GPx in detoxification of H_2O_2 produced by $CoCl_2$. The cells were able to repair the oxidative cellular damage by some cellular defense mechanism(s) that significantly subordinate the amount of free-radical species formed during excessive production of ROS. However, the mitochondrial respiration has been inhibited by the increased ROS formation that induces lipid peroxidation.[61] In the present study, a significantly high intensity of LPO was ascertained after exposure to $CoCl_2$. The failure in cell viability was also found subsequent to the introduction of $CoCl_2$ in both mono- and co-cultured cells.

DOI: 10.1021/acsomega.9b01474
ACS Omega 2019, 4, 20882–20893

During the oxidative stress condition, cells undergo apoptosis and are regulated by a caspase cascade. The signaling pathway of apoptosis is regulated by affirmative and pessimistic regulators, and the equilibrium among these regulators resolves whether the cells undergo apoptosis or survive. The cells survive if the expression of antiapoptotic genes such as Bcl2 and Bcl-xL increases, whereas the cells undergo programmed cell death if the expression of proapoptotic genes Bax, Bad, Bak, and Bid increased. $CoCl_2$ induces the expression of p53 via ROS-mediated DNA damage.[62] p53 upregulates the expression of PUMA, p21, and Bax in response to various stresses. Several reports have shown that p53 moves to the mitochondria in reaction to stress.[63] Subsequently, mitochondrial signaling is triggered, ensuing in the cytoplasmic discharge of cytochrome *c*, pro-caspase-9, etc., which stimulates the activation of caspase-9 and then caspase-3[64,65] HIF-1α can induce apoptosis by increasing the immovability of the artifact of the tumor suppressor gene p53. In oxidative stress or DNA damage, p53 induces apoptosis or growth arrest by regulating Bax or p21, respectively. Several studies have demonstrated both in vivo and in vitro conditions wherein HIF-1α binds straight to the p53 ubiquitin ligase mdm2 and subsequently stabilizes p53.[66] However, other studies showed through obligatory of p53 to the oxygen-dependent degradation domain of HIF1a.

In the current study, we found that the introduction of $CoCl_2$ to both mono and co-cultured cells significantly increased the expression of HIF-1, caspase-3, caspase-9, Bax, and p53 and decreased the expression of Bcl2. Several studies have shown that mitochondrial membrane permeabilization and apoptosis have been initiated by an increase in the level of cytosolic p53 protein after interaction with the mitochondria. It has been proposed that the cytosolic p53 protein induces the proapoptotic gene such as Bax and shifts the antiapoptotic Bcl2 protein.[67] However, the genotoxicity has been prevented by the induction of nuclear p53 protein, which finally leads to controlled cell death.[68,69] Hence, p53 prompts the mitochondrial apoptotic cascade in both types of cultured cells in this study by changing the expression profile of marker genes after exposure to $CoCl_2$.

The benefit of co-culture related to monoculture is its capability to expose the in vivo biology of growth factors, cytokines, and transcriptional regulators either activated or withdrawn in retort to any stress or disease condition. For example, Li et al.[70] reported that the synthesis of IL-6 in the intestinal epithelial cells is directly affected by the monocyte-derived IL-10. This was supposed to pay for disease development through mucin production and cell migration.[70] The co-culture models are used for essential narrative epithelial cell function during disease and regeneration of biological barriers of wound repair. Fibroblasts need to cleave the mature peptide formed between laminin-5-attached basal epithelial cells and the extracellular matrix (ECM) in epidermal tissues. This stimulates integration into ECM to allow stronger epithelial layer attachment.[71] Co-culture has been shown to regenerate the epithelial cells by stimulating the fibroblasts more powerfully in comparison to monolayer culture.[72] This reveals the assistance of fibroblasts in epithelial hurdle renewal and highlights the importance of co-cultures for the swot of wound repair.

The present study demonstrates that apoptosis was decreased in C2C12 cells when they were co-cultured with 3T3-L1 cells in comparison to monocultured C2C12 cells in the presence of $CoCl_2$. The reason may be either activation or repression of many growth factors, cytokines, and transcriptional regulators in co-culture systems.[70] Nevertheless, the possessions of adipocytes on myocytes are still not established and the fundamental mechanism is uncertain. Wang et al.[73] reported that the lipopolysaccharide (LPS)-induced apoptosis has been inhibited in co-culturing of macrophages with DMCs. Apoptosis was induced by LPS in both mono- and co-cultured cells, and they found that the co-cultured cells show 4 times less apoptosis in comparison to monocultured cells in the presence of DMC. On the other hand, C2C12 cells induce apoptosis in 3T3-L1 cells when co-cultured with differentiated C2C12 cells during the hypoxic condition. Chu et al.[74] has reported that the co-culture experiment showed proliferation, cell cycle and differentiation of 3T3-L1 were arrested and apoptosis was induced by differentiated C2C12 myoblast.

CONCLUSIONS

Our study reveals that exposure to $CoCl_2$ significantly induces the expression of hypoxia-inducible factor (HIF-1) in both mono- and co-cultured cell systems. The increased ROS formation leads to oxidative damage in the cells during the hypoxic condition. The ratio of Bcl2/Bax has been reduced due to the increased ROS generation upregulation of p53 gene, and downregulaion of Bcl2 gene. Cytochrome *c* has been released due to alteration in the ratio of Bcl2/Bax, which finally activates caspase-9 and consequently prompts the caspase-3 cascade, leading to apoptosis in both mono- and co-cultured cells. However, the monocultured C2C12 cells respond significantly high toward the hypoxia-induced oxidative stress after exposure to $CoCl_2$. While the co-cultured C2C12 cells also show the oxidative stress toward $CoCl_2$ exposure, the magnitude is lower in comparison to monoculture cells. The co-cultured cells also show the protective potential toward the oxidative stress-mediated cell death to some extent. However, the co-cultured 3T3-L1 cells respond higher toward the hypoxia-induced oxidative stress in comparison to monocultured 3T3-L1 cells.

AUTHOR INFORMATION

Corresponding Author

*E-mail: inho.hwang@jbnu.ac.kr. Phone/Fax: +82-063-270-2605.

ORCID

Sivakumar Allur Subramaniyan: 0000-0002-1354-7780

Author Contributions

[§]V.K.T. and S.A.S. contributed equally to this work.

Notes

The authors declare no competing financial interest.

ACKNOWLEDGMENTS

The authors acknowledge the Rural Development Administration, Republic of Korea, for the financial support under the research program of next generation Biogreen 21 (PJ013169) and also theKorea Institute of Planning and Evaluation for Technology in Food, Agriculture and Forestry (IPET) through Hanwoo Export Program, funded by the Ministry of Agriculture, Food and Rural Affairs (MAFRA) (PN. 618002-5).

DOI: 10.1021/acsomega.9b01474
ACS Omega 2019, 4, 20882−20893

REFERENCES

(1) Semenza, G. L. Targeting HIF-1 for cancer therapy. *Nat. Rev. Cancer* **2003**, *3*, 721−732.

(2) Sivakumar, A. S.; Krishnaraj, C.; Sheet, S.; Rampa, D. R.; Kang, D. R.; Belal, S. A.; Kumar, A.; Hwang, I. H.; Yun, S. I.; Lee, Y. S.; Shim, K. S. Interaction of silver and gold nanoparticles in mammalian cancer: as real topical bullet for wound healing-A comparative study. *In Vitro Cell. Dev. Biol.: Anim.* **2017**, 632−645.

(3) Young, S. D.; Marshall, R. S.; Hill, R. P. Hypoxia induces DNA overreplication and enhances metastatic potential of murine tumor cells. *Proc. Natl. Acad. Sci. U.S.A.* **1988**, *85*, 9533−9537.

(4) Coquelle, A.; Toledo, F.; Stern, S.; Bieth, A.; Debatisse, M. A new role for hypoxia in tumor progression: induction of fragile site triggering genomic rearrangements and formation of complex DMs and HSRs. *Mol. Cell* **1998**, *2*, 259−265.

(5) Reynolds, T. Y.; Rockwell, S.; Glazer, P. M. Genetic instability induced by the tumor microenvironment. *Cancer Res.* **1996**, *56*, 5754−5757.

(6) Hirsilä, M.; Koivunen, P.; Xu, L.; Seeley, T.; Kivirikko, K. I.; Myllyharju, J. Effect of desferrioxamine and metals on the hydroxylases in the oxygen sensing pathway. *FASEB J.* **2005**, *19*, 1308−1310.

(7) Carmeliet, P.; Dor, Y.; Herbert, J. M.; Fukumura, D.; Brusselmans, K.; Dewerchin, M.; Koch, C. J. Role of HIF-1α in hypoxia-mediated apoptosis, cell proliferation and tumour angiogenesis. *Nature* **1998**, *394*, 485.

(8) Moritz, W.; Meier, F.; Stroka, D. M.; Giuliani, M.; Kugelmeier, P.; Nett, P. C.; Lehmann, R.; Candinas, D.; Gassmann, M.; Weber, M. Apoptosis in hypoxic human pancreatic islets correlates with HIF-1α expression. *FASEB J.* **2002**, *16*, 745−757.

(9) Akakura, N.; Kobayashi, M.; Horiuchi, I.; Suzuki, A.; Wang, J.; Chen, J.; Asaka, M. Constitutive expression of hypoxia-inducible factor-1α renders pancreatic cancer cells resistant to apoptosis induced by hypoxia and nutrient deprivation. *Cancer Res.* **2001**, *61*, 6548−6554.

(10) Leonard, S. S.; Harris, G. K.; Shi, X. Metal-induced oxidative stress and signal transduction. *Free Radical Biol. Med.* **2004**, *37*, 1921−1942.

(11) Ke, Q.; Costa, M. Hypoxia-inducible factor-1 (HIF-1). *Mol. Pharmacol.* **2006**, *70*, 1469−1480.

(12) Gilmore, T. D. Introduction to NF-κB: players, pathways, perspectives. *Oncogene* **2006**, *25*, 6680.

(13) Taylor, C. T.; Cummins, E. P. The Role of NF-κB in Hypoxia-Induced Gene Expression. *Ann. N. Y. Acad. Sci.* **2009**, *1177*, 178−184.

(14) Semenza, G. L. HIF-1: mediator of physiological and pathophysiological responses to hypoxia. *J. Appl. Physiol.* **2000**, *88*, 1474−1480.

(15) Wenger, R. H. Mammalian oxygen sensing, signalling and gene regulation. *J. Exp. Biol.* **2000**, *203*, 1253−1263.

(16) Hoppeler, H.; Vogt, M.; Weibel, E. R.; Fluck, M. Response of skeletal muscle mitochondria to hypoxia. *Exp. Physiol.* **2003**, *88*, 109−119.

(17) Archer, S.; Michelakis, E. The mechanism (s) of hypoxic pulmonary vasoconstriction: potassium channels, redox O_2 sensors, and controversies. *News Physiol. Sci.* **2002**, *17*, 131−137.

(18) Chandel, N. S.; McClintock, D. S.; Feliciano, C. E.; Wood, T. M.; Melendez, J. A.; Rodriguez, A. M.; Schumacker, P. T. Reactive oxygen species generated at mitochondrial complex III stabilize hypoxia-inducible factor-1α during hypoxia a mechanism of O2 sensing. *J. Biol. Chem.* **2000**, *275*, 25130−25138.

(19) Goyal, P.; Weissmann, N.; Grimminger, F.; Hegel, C.; Bader, L.; Rose, F.; Fink, L.; et al. Upregulation of NAD (P) H oxidase 1 in hypoxia activates hypoxia-inducible factor 1 via increase in reactive oxygen species. *Free Radical Biol. Med.* **2004**, *36*, 1279−1288.

(20) Atlante, A.; Gagliardi, S.; Minervini, G. M.; Ciotti, M. T.; Marra, E.; Calissano, P. Glutamate neurotoxicity in rat cerebellar granule cells: a major role for xanthine oxidase in oxygen radical formation. *J. Neurochem.* **1997**, *68*, 2038−2045.

(21) Zou, W.; Zeng, J.; Zhuo, M.; Xu, W.; Sun, L.; Wang, J.; Liu, X. Involvement of caspase-3 and p38 mitogen-activated protein kinase in cobalt chloride-induced apoptosis in PC12 cells. *J. Neurosci. Res.* **2002**, *67*, 837−843.

(22) Chen, L.; Liu, L.; Yin, J.; Luo, Y.; Huang, S. Hydrogen peroxide-induced neuronal apoptosis is associated with inhibition of protein phosphatase 2A and 5, leading to activation of MAPK pathway. *Int. J. Biochem. Cell Biol.* **2009**, *41*, 1284−1295.

(23) Jung, J. Y.; Kim, W. J. Involvement of mitochondrial-and Fas-mediated dual mechanism in CoCl 2-induced apoptosis of rat PC12 cells. *Neurosci. Lett.* **2004**, *371*, 85−90.

(24) Cao, Y. J.; Shibata, T.; Rainov, N. G. Hypoxia-inducible transgene expression in differentiated human NT2N neurons−a cell culture model for gene therapy of postischemic neuronal loss. *Gene Ther.* **2001**, *8*, 1357.

(25) Chen, L.; Liu, L.; Luo, Y.; Huang, S. MAPK and mTOR pathways are involved in cadmium-induced neuronal apoptosis. *J. Neurochem.* **2008**, *105*, 251−261.

(26) Nusuetrong, P.; Yoshida, M.; Tanitsu, M. A.; Kikuchi, H.; Mizugaki, M.; Shimazu, K. I.; Pengsuparp, T.; Meksuriyen, D.; Oshima, Y.; Nakahata, N. Involvement of reactive oxygen species and stress-activated MAPKs in satratoxin H-induced apoptosis. *Eur. J. Pharmacol.* **2005**, *507*, 239−246.

(27) Wu, D. C.; Re, D. B.; Nagai, M.; Ischiropoulos, H.; Przedborski, S. The inflammatory NADPH oxidase enzyme modulates motor neuron degeneration in amyotrophic lateral sclerosis mice. *Proc. Natl. Acad. Sci. U.S.A.* **2006**, *103*, 12132−12137.

(28) Kim, S. D.; Moon, C. K.; Eun, S. Y.; Ryu, P. D.; Jo, S. A. Identification of ASK1, MKK4, JNK, c-Jun, and caspase-3 as a signaling cascade involved in cadmium-induced neuronal cell apoptosis. *Biochem. Biophys. Res. Commun.* **2005**, *328*, 326−334.

(29) Valencia, A.; Morán, J. Reactive oxygen species induce different cell death mechanisms in cultured neurons. *Free Radical Biol. Med.* **2004**, *36*, 1112−1125.

(30) Green, K. N.; Peers, C. Divergent pathways account for two distinct effects of amyloid β peptides on exocytosis and Ca^{2+} currents: involvement of ROS and NF-κB. *J. Neurochem.* **2002**, *81*, 1043−1051.

(31) Wu, M. H.; Huang, S. B.; Lee, G. B. Microfluidic cell culture systems for drug research. *Lab Chip* **2010**, *10*, 939−956.

(32) Berin, M. C.; McKay, D. M.; Perdue, M. H. Immune-epithelial interactions in host defense. *Am. J. Trop. Med. Hyg.* **1999**, *60*, 16−25.

(33) Muthuraman, P. Effect of coculturing on the myogenic and adipogenic marker gene expression. *Appl. Biochem. Biotechnol.* **2014**, *173*, 571−578.

(34) Choi, S. H.; Chung, K. Y.; Johnson, B. J.; Go, G. W.; Kim, K. H.; Choi, C. W.; Smith, S. B. Co-culture of bovine muscle satellite cells with preadipocytes increases PPARγ and C/EBPβ gene expression in differentiated myoblasts and increases GPR43 gene expression in adipocytes. *J. Nutr. Biochem.* **2013**, *24*, 539−543.

(35) Yan, J.; Gan, L.; Yang, H.; Sun, C. The proliferation and differentiation characteristics of co-cultured porcine preadipocytes and muscle satellite cells in vitro. *Mol. Biol. Rep.* **2013**, *40*, 3197−3202.

(36) Subramaniyan, S. A.; Kim, S.; Hwang, I. Cell-Cell Communication Between Fibroblast and 3T3-L1 Cells Under Co-culturing in Oxidative Stress Condition Induced by H_2O_2. *Appl. Biochem. Biotechnol.* **2016**, *180*, 668−681.

(37) Kumar, V.; Gupta, A. K.; Shukla, R. K.; Tripathi, V. K.; Jahan, S.; Pandey, A.; Srivastava, A.; Agrawal, M.; Yadav, S.; Khanna, V. K.; Pant, A. B. Molecular Mechanism of Switching of TrkA/p75NTR Signaling in Monocrotophos Induced Neurotoxicity. *Sci. Rep.* **2015**, *5*, No. 14038.

(38) Ferri, P.; Barbieri, E.; Burattini, S.; Guescini, M.; D'Emilio, A.; Biagiotti, L.; Del Grande, P.; De Luca, A.; Stocchi, V.; Falcieri, E. Expression and subcellular localization of myogenic regulatory factors during the differentiation of skeletal muscle C2C12 myoblasts. *J. Cell. Biochem.* **2009**, *108*, 1302−1317.

DOI: 10.1021/acsomega.9b01474
ACS Omega 2019, 4, 20882−20893

(39) Sun, X.; Zemel, M. B. Calcitriol and calcium regulate cytokine production and adipocyte−macrophage cross-talk. *J. Nutr. Biochem.* **2008**, *19*, 392−399.
(40) Pant, A. B.; Agarwal, A. K.; Sharma, V. P.; Seth, P. K. In vitro cytotoxicity evaluation of plastic biomedical devices. *Hum. Exp. Toxicol.* **2001**, *20*, 412−417.
(41) Kashyap, M. P.; Singh, A. K.; Kumar, V.; Tripathi, V. K.; Srivastava, R. K.; Agrawal, M.; Khanna, V. K.; Yadav, S.; Jain, S. K.; Pant, A. B. Monocrotophos induced apoptosis in PC12 cells: role of xenobiotic metabolizing cytochrome P450s. *PLoS One* **2011**, *6*, No. e17757.
(42) Vivek, S. D.; Beatty, S. E.; Morgan, R. M. Customer engagement: Exploring customer relationships beyond purchase. *J. Mark. Theory Pract.* **2012**, *20*, 122−146.
(43) Siddiqui, M. A.; Kashyap, M. P.; Kumar, V.; Al-Khedhairy, A. A.; Musarrat, J.; Pant, A. B. Protective potential of trans-resveratrol against 4-hydroxynonenal induced damage in PC12 cells. *Toxicol. In Vitro* **2010**, *24*, 1592−1598.
(44) Kumar, V.; Tripathi, V. K.; Jahan, S.; Agrawal, M.; Pandey, A.; Khanna, V. K.; Pant, A. B. Lead intoxication synergies of the ethanol-induced toxic responses in neuronal cells—PC12. *Mol. Neurobiol.* **2015**, *52*, 1504−1520.
(45) Seta, K. A.; Millhorn, D. E. Functional genomics approach to hypoxia signalling. *J. Appl. Physiol.* **2004**, *96*, 765−773.
(46) Kietzmann, T.; Knabe, W.; Schmidt-Kastner, R. Hypoxia and hypoxia-inducible factor modulated gene expression in brain: involvement in neuroprotection and cell death. *Eur. Arch. Psychiatry Clin. Neurosci.* **2001**, *251*, 170−178.
(47) Kietzmann, T.; Fandrey, J.; Acker, H. Oxygen radicals as messengers in oxygen-dependent gene expression. *News Physiol. Sci.* **2000**, *15*, 202−208.
(48) Jejurikar, S. S.; Kuzon, W. M. Satellite cell depletion in degenerative skeletal muscle. *Apoptosis* **2003**, *8*, 573−578.
(49) Kawanishi, S.; Hiraku, Y.; Murata, M.; Oikawa, S. The role of metals in site-specific DNA damage with reference to carcinogenesis1, 2. *Free Radical Biol. Med.* **2002**, *32*, 822−832.
(50) Lee, M.; Lapham, A.; Brimmell, M.; Wilkinson, H.; Packham, G. Inhibition of proteasomal degradation of Mcl-1 by cobalt chloride suppresses cobalt chloride-induced apoptosis in HCT116 colorectal cancer cells. *Apoptosis* **2008**, *13*, 972−982.
(51) Jung, J. Y.; Roh, K. H.; Jeong, Y. J.; Kim, S. H.; Lee, E. J.; Kim, M. S.; Oh, W. M.; Oh, H. K.; Kim, W. J. Estradiol protects PC12 cells against CoCl2-induced apoptosis. *Brain Res. Bull.* **2008**, *76*, 579−585.
(52) Bell, E. L.; Klimova, T. A.; Eisenbart, J.; Schumacker, P. T.; Chandel, N. S. Mitochondrial reactive oxygen species trigger hypoxia-inducible factor-dependent extension of the replicative life span during hypoxia. *Mol. Cell. Biol.* **2007**, *27*, 5737−5745.
(53) Guzy, R. D.; Hoyos, B.; Robin, E.; Chen, H.; Liu, L.; Mansfield, K. D.; Simon, M. C.; Hammerling, U.; Schumacker, P. T. Mitochondrial complex III is required for hypoxia-induced ROS production and cellular oxygen sensing. *Cell Metab.* **2005**, *1*, 401−408.
(54) Fandrey, J.; Frede, S.; Jelkmann, W. Role of hydrogen peroxide in hypoxia-induced erythropoietin production. *Biochem. J.* **1994**, *303*, 507−510.
(55) Vaux, E. C.; Metzen, E.; Yeates, K. M.; Ratcliffe, P. J. Regulation of hypoxia-inducible factor is preserved in the absence of a functioning mitochondrial respiratory chain. *Blood* **2001**, *98*, 296−302.
(56) Agani, F. H.; Pichiule, P.; Chavez, J. C.; LaManna, J. C. The role of mitochondria in the regulation of hypoxia-inducible factor 1 expression during hypoxia. *J. Biol. Chem.* **2000**, *275*, 35863−35867.
(57) Schroedl, C.; McClintock, D. S.; Budinger, G. S.; Chandel, N. S. Hypoxic but not anoxic stabilization of HIF-1α requires mitochondrial reactive oxygen species. *Am. J. Physiol.: Lung Cell. Mol. Physiol.* **2002**, *283*, L922−L931.
(58) Callapina, M.; Zhou, J.; Schmid, T.; Köhl, R.; Brüne, B. NO restores HIF-1α hydroxylation during hypoxia: role of reactive oxygen species. *Free Radical Biol. Med.* **2005**, *39*, 925−936.
(59) Wartenberg, M.; Ling, F. C.; Müdchen, M.; Klein, F.; Acker, H.; Gassmann, M.; Petrat, K.; et al. Regulation of the multidrug resistance transporter P-glycoprotein in multicellular tumor spheroids by hypoxia-inducible factor (HIF-1) and reactive oxygen species. *FASEB J.* **2003**, *17*, 503−505.
(60) Shukla, D.; Saxena, S.; Jayamurthy, P.; Sairam, M.; Singh, M.; Jain, S. K.; Bansal, A.; Ilavazaghan, G. Hypoxic preconditioning with cobalt attenuates hypobaric hypoxia-induced oxidative damage in rat lungs. *High Alt. Med. Biol.* **2009**, *10*, 57−69.
(61) Flora, S. J.; Gautam, P.; Kushwaha, P. Lead and ethanol co-exposure lead to blood oxidative stress and subsequent neuronal apoptosis in rats. *Alcohol Alcohol.* **2012**, *47*, 92−101.
(62) Liu, B.; Chen, Y.; Clair, D. K. S. ROS and p53: a versatile partnership. *Free Radical Biol. Med.* **2008**, *44*, 1529−1535.
(63) Vaseva, A. V.; Moll, U. M. The mitochondrial p53 pathway. *Biochim. Biophys. Acta, Bioenerg.* **2009**, *1787*, 414−420.
(64) Kashyap, M. P.; Singh, A. K.; Siddiqui, M. A.; Kumar, V.; Tripathi, V. K.; Khanna, V. K.; Yadav, S.; Jain, S. K.; Pant, A. B. Caspase cascade regulated mitochondria mediated apoptosis in monocrotophos exposed PC12 cells. *Chem. Res. Toxicol.* **2010**, *23*, 1663−1672.
(65) Leist, M.; Jaattela, M. Four deaths and a funeral: from caspases to alternative mechanisms. *Nat. Rev. Mol. Cell Biol.* **2001**, *2*, 589.
(66) Chen, D.; Li, M.; Luo, J.; Gu, W. Direct interactions between HIF-1α and Mdm2 modulate p53 function. *J. Biol. Chem.* **2003**, *278*, 13595−13598.
(67) Galluzzi, L.; Morselli, E.; Kepp, O.; Tajeddine, N.; Kroemer, G. Targeting p53 to mitochondria for cancer therapy. *Cell Cycle* **2008**, *7*, 1949−1955.
(68) Bargonetti, J.; Manfredi, J. J. Multiple roles of the tumor suppressor p53. *Curr. Opin. Oncol.* **2002**, *14*, 86−91.
(69) Cui, Q.; Yu, J. H.; Wu, J. N.; Tashiro, S. I.; Onodera, S.; Minami, M.; Ikejima, T. P53-mediated cell cycle arrest and apoptosis through a caspase-3-independent, but caspase-9-dependent pathway in oridonin-treated MCF-7 human breast cancer cells. *Acta Pharmacol. Sin.* **2007**, *28*, 1057.
(70) Li, Y. Y.; Chang, J. W. C.; Hsieh, L. L.; Yeh, K. Y. Neutralization of interleukin (IL)-10 released by monocytes/macrophages enhances the up-regulatory effect of monocyte/macrophage-derived IL-6 on expressions of IL-6 and MUC1, and migration in HT-29 colon cancer cells. *Cell. Immunol.* **2010**, *265*, 164−171.
(71) Elkhal, A.; Tunggal, L.; Aumailley, M. Fibroblasts contribute to the deposition of laminin 5 in the extracellular matrix. *Exp. Cell Res.* **2004**, *296*, 223−230.
(72) Seltana, A.; Basora, N.; Beaulieu, J. F. Intestinal epithelial wound healing assay in an epithelial−mesenchymal co-culture system. *Wound Repair Regener.* **2010**, *18*, 114−122.
(73) Wang, Y.; Tan, L.; Jin, J.; Sun, H.; Chen, Z.; Tan, X.; Shi, C. Non-cultured dermal-derived mesenchymal cells attenuate sepsis induced by cecal ligation and puncture in mice. *Sci. Rep.* **2015**, *5*, No. 16973.
(74) Chu, W.; Wei, W.; Yu, S.; Han, H.; Shi, X.; Sun, W.; Gao, Y.; Zhang, L.; Chen, J. C2C12 myotubes inhibit the proliferation and differentiation of 3T3-L1 preadipocytes by reducing the expression of glucocorticoid receptor gene. *Biochem. Biophys. Res. Commun.* **2016**, *472*, 68−74.

DOI: 10.1021/acsomega.9b01474
ACS Omega 2019, 4, 20882−20893